


Onset of Lagrangian chaos: From fractal power spectrum to the absolutely continuous one

Rafil V. Sagitov ^{*}*Perm State University, 614990 Perm, Russia*Igor I. Wertgeim [†]*Institute of Continuous Media Mechanics, 614013 Perm, Russia*Michael A. Zaks [‡]*Institut für Physik, Humboldt-Universität zu Berlin, 12489 Berlin, Germany*

(Received 20 June 2023; accepted 20 December 2023; published 18 January 2024)

We study transition to chaotic advection in the fluid motion across a plane rectangular domain with periodic boundary conditions. The flow, induced by a combination of time-independent force with constant pumping in both spatial directions, is equivalent to dynamics on the surface of a 2-torus. At considered force amplitudes, the stationary flow pattern includes the global drift and the localized vortices encircled by separatrices of stagnation points. If the Eulerian velocity field is time-independent and rotation number on the torus, controlled by pumping intensities, is irrational, then the power spectrum of the Lagrangian observables is singular continuous (fractal) and the autocorrelation function of velocity displays no ultimate decay. As the increase of the force destabilizes the stationary flow and replaces it by periodically oscillating velocity field, singularities in the numerically evaluated spectrum disappear, whereas temporal correlations vanish after a certain time interval.

DOI: [10.1103/PhysRevFluids.9.014401](https://doi.org/10.1103/PhysRevFluids.9.014401)

I. INTRODUCTION

Two observers of the same velocity field, the first one (traditionally called “the Eulerian” observer) measuring its characteristics at a fixed spatial location, and the second (respectively, “the Lagrangian”) one traveling on a passive particle advected by that field, can report remarkably different pictures. The difference is seen already when the velocity field is stationary in time: measurements of the Eulerian observer invariably return constant values whereas the Lagrangian observer can experience regular or irregular sequences of accelerations and slowdowns. If the stationary velocity in question is the velocity of an incompressible fluid, and molecular diffusion is neglected, the cavity filled with this fluid turns into the phase space of a volume-preserving dynamical system, and paths of the Lagrangian tracers become phase trajectories. In three-dimensional stationary flows, patterns of streamlines can be chaotic [1]; this phenomenon is known as chaotic advection [2] or Lagrangian turbulence [3].

Below, we restrict ourselves to two-dimensional fluid motions. In a plane stationary flow confined to a finite domain, a generic streamline is closed, hence a motion of a tracer advected along it

*sagitovrv@mail.ru

†wertg@icmm.ru

‡zaks@physik.hu-berlin.de

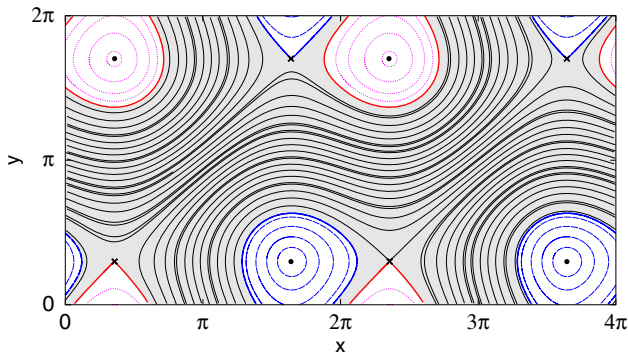


FIG. 1. Mixed phase space of a conservative flow on a 2-torus in presence of stagnation points. Phase portrait for Eq. (5) at parameter values (parameters are introduced further in the text): $l_x = 2$, $l_y = 1$, $\nu = 1$, $\alpha = 1$, $\beta = (\sqrt{5} - 1)/2$, $f = 2$. Gray background: global drift. White background: localized vortices. Filled circles: elliptic stagnation points. Crosses: hyperbolic stagnation points.

is periodic. More involved temporal dynamics of advected particles arises in the case of periodic boundary conditions: there, a stationary plane flow of incompressible fluid is equivalent to the conservative flow on the surface of a 2-torus. If this flow has a rational rotation number, all streamlines are closed and the motion of each advected tracer is periodic in time. For irrational rotation numbers, the overall picture depends on the absence/presence of stagnation points in the flow pattern. Without such points, the motion is ergodic, every streamline is dense on the whole toroidal surface, and temporal dynamics is a quasiperiodic rotation around the torus. In the presence of stagnation points, the phase space is mixed (Fig. 1): separated into the “localized” vortices (regions filled with closed streamlines and encircled by separatrices of the saddle points), and the ergodic “global” component outside the vortices where every streamline is nonclosed and dense. Note that temporal dynamics of tracers in the global component of the flow is more complicated than conventional quasiperiodicity: accumulated effect of slowdowns during repeated passages close to the stagnation points manifests itself in decorrelation and weak mixing. This widespread kind of behavior, intermediate between chaos (which is impossible in the two-dimensional phase space) and ordered periodic or quasiperiodic motion, is known as “dynamics with singular continuous power spectrum” [4].

II. TYPES OF POWER SPECTRA AS CLUES TO DYNAMICS

As the name suggests, the phenomenon can be traced back to the composition of the Fourier spectra, in this case, spectra of the Lagrangian observables like velocity of advected particles. Fourier spectra and their counterparts—the correlation functions—have a long tradition as criteria for nontrivial dynamics. Remarkably, the first quantitative studies of the transition to turbulence in a flow between rotating concentric cylinders [5] and in thermal convection [6] were based on the Fourier spectra of velocity; in those experiments, measurements were performed not for fixed tracers but at fixed locations, giving evidence for the Eulerian turbulence. Below we demonstrate how the loss of stationarity—onset of time dependence—in the velocity field transforms the spectra of the Lagrangian observables from the singular continuous into the more familiar absolutely continuous ones.

In general, spectral measure is uniquely decomposable into the discrete and continuous components; within the latter, a further dichotomy is made between absolutely continuous (with respect to the Lebesgue measure) and singular continuous spectrum [7]. Depending on the problem, any one or two components can be absent. Formally, the calculation of the Fourier spectrum assumes integration (summation) over the sample of infinite length; in experiments, conclusions on the spectral

type must be drawn from finite spectral sums. Computationally, three spectral types are discernible through different behavior of Fourier sums under growth of the sample length L . In the context of time-dependent observables, the variable of the Fourier transform is the frequency, denoted below by ω . For the values of ω belonging to the absolutely continuous spectral component, spectral sums $S(\omega, L)$ converge to finite limits $S(\omega)$. In contrast, the discrete (atomic) spectral component is built of the Dirac delta-functions; at the corresponding values of ω , spectral sums grow proportionally to L . Finally, the singular continuous (fractal) spectral component supports the infinite set of singularities for which the spectral sums under varying L either grow sublinearly (that is, slower than for a delta function) or oscillate. Here, increase of L yields no convergent power spectrum; instead, growth of the sample ensures infinite fragmentation of the spectral curve, with more and more emerging peaks and troughs. In the context of physics, singular continuous power spectra (with regards to the spatial Fourier transform) were reported in [8] as “intermediate between quasiperiodic and random;” later their occurrence was detected in certain classes of deterministic dynamical systems [4]. Conventionally, discrete spectrum is an indicator of regular dynamics whereas the absolutely continuous one is a hallmark of chaos, turbulence, randomness. Accordingly, motions with singular continuous spectra are neither perfectly ordered nor strongly disordered and have a certain intermediate position; although they may seem exotic, for the considered hydrodynamical context the set which supports them in the parameter space has a positive measure.

III. EXAMPLE: A STEADY VISCOUS FLOW WITH MEAN DRIFT IN A RECTANGLE WITH PERIODIC BOUNDARY CONDITIONS

An example of steady viscous flow with singular continuous power spectrum was suggested in [9]. The two-dimensional time-independent velocity field was induced on a square with periodic boundary conditions (that is, on a 2-torus) by a force, periodic along two spatial directions; rotation number was controlled by constant pumping in both directions. With the force strong enough to sustain stationary eddies in the flow with irrational rotation number, autocorrelation of the velocity for an advected particle acquired the roughly log-periodic pattern, characteristic for flows with singular continuous power spectra. Below we demonstrate that the oscillatory hydrodynamical instability of this flow pattern leads to the onset of chaotic advection and makes the Fourier spectrum absolutely continuous.

Setup: incompressible fluid with kinematic viscosity ν and density ρ , obeying the Navier-Stokes equations

$$\begin{aligned} \frac{\partial \mathbf{v}}{\partial t} + (\mathbf{v} \cdot \nabla) \mathbf{v} &= -\frac{\nabla P}{\rho} + \nu \nabla^2 \mathbf{v} + \mathbf{F}, \\ \nabla \cdot \mathbf{v} &= 0 \end{aligned} \quad (1)$$

flows over the rectangle $0 \leq x \leq 2\pi l_x$, $0 \leq y \leq 2\pi l_y$, with l_x and l_y being positive integers. Here \mathbf{v} and P are, respectively, the velocity and the pressure; the plane force $\mathbf{F} = (f \sin y, f \sin x)$ is periodic in space, and time independent. The structure of the forcing term reminds of the Kolmogorov flow [10]; experimental implementation of spatially periodic force by placing arrays of electrodes into the thin layers of conducting fluid was described in [11,12].

Spatial periodicity of the velocity field,

$$\mathbf{v}(x, y) = \mathbf{v}(x + 2\pi l_x, y) = \mathbf{v}(x, y + 2\pi l_y), \quad (2)$$

implies that the opposite borders of the periodicity domain can be pairwise adjusted: the domain can be regarded as a 2-torus. Further, we prescribe the fixed nonzero mean drift in both directions across the domain, parametrizing it by two drift rates α and β :

$$\frac{1}{2\pi l_y} \int_0^{2\pi l_y} v_x dy = \alpha, \quad \frac{1}{2\pi l_x} \int_0^{2\pi l_x} v_y dx = \beta. \quad (3)$$

On introducing in the standard way the stream function $\Psi(x, y)$ by relations $v_x = \partial\Psi/\partial y$, $v_y = -\partial\Psi/\partial x$, the Navier-Stokes equations (1) are rewritten as

$$\frac{\partial \Delta \psi}{\partial t} + \frac{\partial \psi}{\partial y} \frac{\partial \Delta \psi}{\partial x} - \frac{\partial \psi}{\partial x} \frac{\partial \Delta \psi}{\partial y} - \nu \Delta \Delta \psi = f(\cos y - \cos x). \quad (4)$$

Conditions (3) for the flow rates turn into $\Psi(2\pi l_x, y) - \Psi(0, y) = -2\pi\beta l_x$ and $\Psi(x, 2\pi l_y) - \Psi(x, 0) = 2\pi\alpha l_y$. Due to the periodicity of the velocity field along both coordinates, the stream function can be written as $\Psi(x, y) = \alpha y - \beta x + \Phi(x, y)$, where $\Phi(x, y)$ is $2\pi l_x$ periodic with respect to x , and $2\pi l_y$ periodic with respect to y . For steady flow patterns on a torus, it makes sense to characterize each streamline (isoline of Ψ) by the rotation number: the tangent of the mean inclination of the streamline to the coordinate axis. It is straightforward to see that in the described geometry of the flow, rotation number is the same for all streamlines winding around the torus; it equals α/β (for closed streamlines localized inside the periodicity domain, rotation number is zero).

The steady solution of Eq. (4),

$$\Psi = \alpha y - \beta x + \frac{f \sin(x - \phi_1)}{\sqrt{\alpha^2 + \nu^2}} - \frac{f \sin(y - \phi_2)}{\sqrt{\beta^2 + \nu^2}}, \quad (5)$$

with $\phi_1 = -\arctan \frac{\nu}{\alpha}$, $\phi_2 = -\arctan \frac{\nu}{\beta}$ renders the stationary velocity field [9]

$$\begin{aligned} \dot{x} = v_x &= \alpha - \frac{f \cos(y - \phi_2)}{\sqrt{\beta^2 + \nu^2}} \\ \dot{y} = v_y &= \beta - \frac{f \cos(x - \phi_1)}{\sqrt{\alpha^2 + \nu^2}}. \end{aligned} \quad (6)$$

The conservative dynamical system (6) governs the motion of the particles, advected by the stationary flow pattern (5). For the vector field (6), the entire flow domain can be viewed as a rectangle covered by $l_x \times l_y$ squares with the side length 2π .

Without forcing, the streamlines are straight, and the velocity is uniform: this is the trivial flow on the 2-torus with rotation number α/β . At nonzero f the streamlines are curved; for $f < f_{sc} = \sqrt{\alpha^2 \beta^2 + \nu^2} \max(\alpha^2, \beta^2)$ and irrational α/β every streamline is dense on the torus, and the motion along the streamline is ergodic. At $f = f_{sc}$ the saddle-center bifurcation creates in each $2\pi \times 2\pi$ square two pairs of stagnation points. Elliptic points (centers) are surrounded by vortex-shaped continua of closed streamlines, encircled by separatrices of hyperbolic stagnation points (saddles); these vortices form the localized component of the flow pattern (Fig. 1).

Within the global component (i.e., outside the vortices) every streamline is dense. In the course of time, advected particles repeatedly come arbitrarily close to the saddle points and depart again; the cumulative effect of slowdowns and subsequent accelerations is decorrelation. The hitherto discrete Fourier spectrum of velocity becomes singular continuous [9]. A characteristic illustration in the top left panel of Fig. 2 can be viewed as an instantaneous snapshot of the nonconvergent computation procedure for the fractal spectrum: every further increase of the sample length discloses new singularities and creates new extrema on this infinitely fragmented curve.

Notably, for plane steady flows across domains with periodic boundary conditions, existence of singular continuous spectra for Lagrangian observables is a common phenomenon. Indeed, it requires two conditions: irrational rotation number and presence of stagnation points. Flows fulfilling the second condition are structurally stable. As for the first one, although each separate irrational rotation number is structurally unstable, taken together the irrationals form a set of full measure.

In the canonical Kolmogorov flow, as well as in its generalizations, the basic stationary flow pattern becomes unstable at high forcing amplitude and is replaced by various secondary and ternary states (see, e.g., [13–15] and references therein). Notably, the longwave perturbations are often the most dangerous ones [16]. Numerical analysis of Eq. (4) linearized near the stationary flow pattern

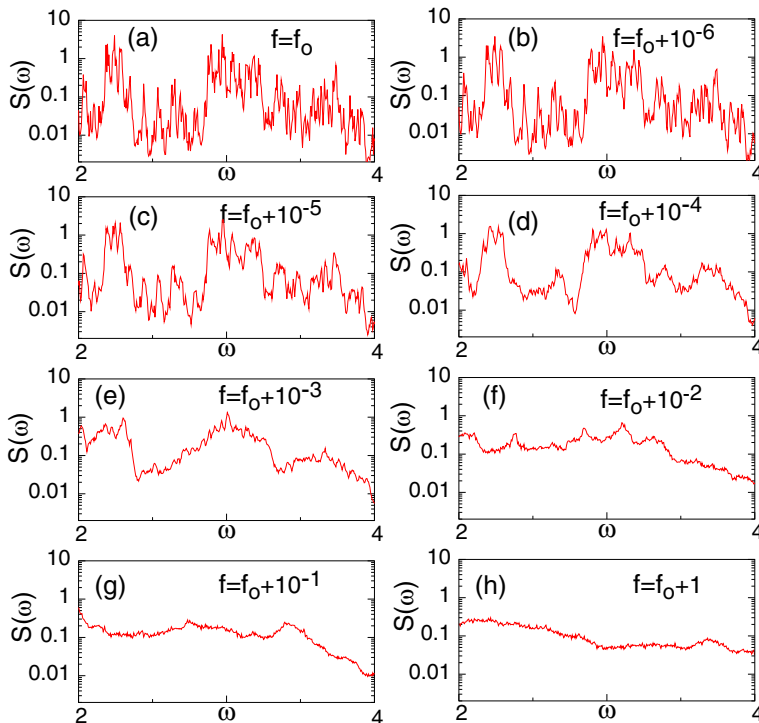


FIG. 2. Smoothing of the shape of the power spectrum for the component v_x of velocity of the Lagrangian tracer close to the onset at f_o of the oscillatory instability of the stationary flow pattern. Each curve is the average over ~ 300 periodograms from the single trajectory, obtained by numerical integration of Eq. (4) and divided into segments with 2^{16} datapoints/segment. Parameters: $l_x = 2$, $l_y = 1$, $\nu = 1$, $\alpha = 1$, $\beta = (\sqrt{5} - 1)/2$, $f_o = 2.712561$.

(5) has disclosed that in the square domain with the size equal to the spatial period of the force (that is, $l_x = l_y = 1$), this pattern remains stable at all tested forcing amplitudes f ; regardless of f , the flow regime with singular continuous Fourier spectrum of velocity is attracting. If, however, the length of any size of the domain exceeds the period of the force, disturbances with the longer wavelength are enabled, and there exists a critical value of the forcing amplitude f beyond which the stationary pattern (5) loses stability. Description of various bifurcation scenarios and secondary flows in this system is given in [15]. Below, we restrict ourselves to the region of the parameter space of Eq. (4) in which the primary instability of (5) is oscillatory and, in terms of the Eulerian variables, the supercritical Andronov-Hopf bifurcation occurs: birth of the limit cycle in the phase space. The flow pattern becomes time dependent; for Lagrangian observables, in accordance with the general formalism [3], this leads to the onset of chaotic advection. Above the destabilization, the continuum of closed streamlines inside every localized vortex generates the set of the Kolmogorov-Arnold-Moser (KAM) tori; in the global component, metamorphoses of trajectories depend on the rotation number. If the latter is rational, the global component becomes filled by KAM-tori as well; if it is irrational, separatrices of the perturbed saddle points intersect transversely and form the heteroclinic web: a skeleton of the newborn chaotic set [17]. Just above the onset of time dependence, the distinction between the global and the localized dynamics persists: the KAM-tori serve as barriers, obstructing transport in the $(2 + 1)$ -dimensional phase space. As f is further raised, more and more tori break up, so that finally the localized component shrinks and the whole area of the domain becomes accessible to all advected tracers. Leaving the detailed description of the transitions to the

subsequent paper [18], we focus on changes in spectral and correlational properties of Lagrangian observables.

IV. TRANSFORMATION OF THE FOURIER SPECTRUM

We start with the power spectrum, given for the segment of the length N from equidistant time series ξ_j by $S(\omega) = \langle |\sum_{j=j_0}^{j_0+N-1} \xi_j e^{ij\omega}|^2 \rangle$, where averaging is performed with respect to the initial position j_0 . Initial conditions are taken inside the ergodic global component.

For numerical studies we take the domain of the length 4π and width 2π ; accordingly, $l_x = 2$ and $l_y = 1$. We fix viscosity at $\nu = 1$ and impose the mean drift rates $\alpha = 1$, $\beta = (\sqrt{5} - 1)/2$ so that on the torus the rotation number α/β equals the inverse golden mean.¹ For these parameter values the localized vortices arise on the background of the global drift at $f_{sc} = 1.17557$, the oscillatory instability of the stationary flow pattern (5) occurs at $f_o = 2.712561$, and the last localized vortices are flooded by $f_{fl} \approx 3.07$. Summary of dynamics:

(i) For $|f| < f_{sc}$ stagnation points are absent, the motion of tracers is quasiperiodic and ergodic, the power spectrum of velocity is discrete.

(ii) For $f_{sc} < |f| < f_o$ the phase space is separated, with velocity spectrum for nonlocalized particles being singular continuous.

(iii) For $f_o < |f| < f_{fl}$ the phase space stays separated, but the spectrum is absolutely continuous.

(iv) Finally, for $|f| > f_{fl}$ ergodicity is restored.

Figure 2 illustrates, for the frequency range $2 < \omega < 4$, the changes in the shape of the spectral curve that accompany the growth of the forcing amplitude f . Panel (a) corresponds to stationary flow pattern on the verge of instability and shows a snapshot in the successive buildup of the singular continuous spectrum. The picture changes beyond the threshold f_o of the oscillatory instability: the Fourier spectrum becomes absolutely continuous, and the spectral sums converge to the smooth (albeit still fragmented) curve $S(\omega)$ with finite length.

The further from the threshold, the smoother the curve $S(\omega)$. Sufficiently far beyond f_o , remnants of the singularities disappear, and the curve acquires the relatively uncomplicated shape, characteristic for well-developed chaos. To quantify fragmentation of the computed spectrum, we use the total sum of increments of spectral sums between the neighboring frequency values $\Sigma_v = \sum_{j_0 > 1}^{j_0+N} |S(\omega_j) - S(\omega_{j-1})|$, at the resolution of the curve $N = 2^{16}$. At $f_{sc} < f \leq f_o$ the spectrum is singular continuous, and Σ_v is unbounded. As the forcing decreases to f_o from above, the sum of increments diverges; numerics indicates the power law dependence: $\Sigma_v(f) \sim (f - f_o)^{-0.21}$ [Fig. 3(a)].

V. AUTOCORRELATION OF VELOCITY AND ITS METAMORPHOSES

Obeying the Wiener-Khinchin theorem, the power spectrum of a process is interrelated with its autocorrelation function. Accordingly, transition of the former from singular continuous to the absolutely continuous state is reflected by changes in the pattern of the autocorrelation. The normalized autocorrelation function of the velocity component v_x is

$$C(\tau) = \frac{\langle v_x(t)v_x(t+\tau) \rangle - \langle v_x(t) \rangle^2}{\langle v_x^2(t) \rangle - \langle v_x(t) \rangle^2}, \quad (7)$$

where averaging is performed with respect to the initial point of the trajectory. Maxima of autocorrelation are attained at the values of the argument τ at which the velocity values $v_x(t)$ and

¹Other irrational values of α/β would do as well, but the periodic representation of the golden mean as a continuous fraction seems especially suitable for a demonstration of gradual transformations in the autocorrelation of the velocity of tracers, see Sec. V below.

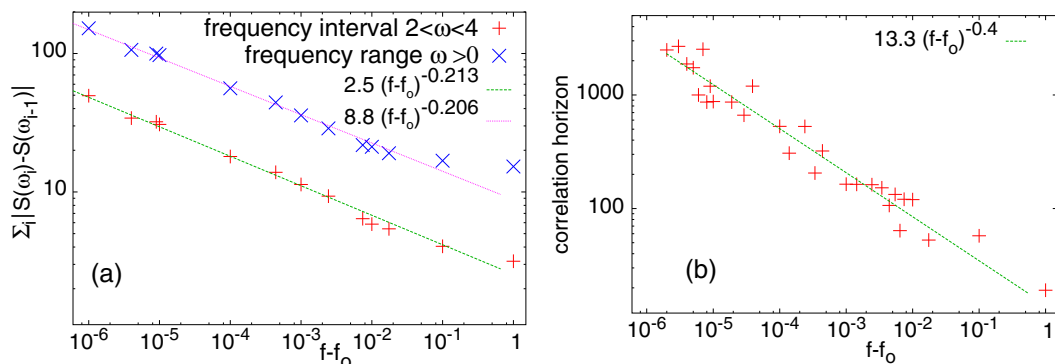


FIG. 3. (a) Divergence of the sum of increments for the spectral curve $S(\omega)$. (b) Correlation horizon for $c_0 = 0.04$ beyond the threshold of oscillatory instability.

$v_x(t + \tau)$ nearly coincide; since the velocity value, in its turn, is rigidly related by Eq. (6) to the position of the fluid particle on the torus, the maxima correspond to typical time intervals of length τ after which the noticeable part of the tracers at $t + \tau$ returns to their positions at time t . For an irrational rotation number, such close returns occur at the values of τ that are proportional to the denominators of rational approximations to this number. In case of the golden mean, such denominators form the famous sequence of Fibonacci numbers $\{F_n\}$ with $F_n = F_{n-2} + F_{n-1}$; several first F_n are 1, 1, 2, 3, 5, 8, ...; the progression grows asymptotically at a rate $(\sqrt{5} + 1)/2$. Notably, the subsequent returns occur in the alternating way: if, say, the return after five rotations around the torus happens on the left side from the initial point, the next close return occurs on the right side after eight rotations (and is closer than that after five rotations). Therefore, for a quasiperiodic flow on the torus with the appropriate rotation number, we can expect the sequence of autocorrelation maxima at the time values proportional to F_n ; for the time axis shown in the logarithmic scale, the maxima should form the approximately equidistant lattice. For the autocorrelation normalized in accordance with (7), the height of the maxima should asymptotically tend to 1. Quasiperiodicity requires absence of states of equilibrium (in terms of the fluid motion, of stagnation points) on the surface of the torus. If stagnation points are present in the flow pattern, the flow is not perfectly quasiperiodic: slowdowns of tracers during repeated passages near the stagnation points give rise to a certain decorrelation [9], so that the autocorrelation maxima, albeit still present and visible, become distinctly lower than 1.

Figure 4 shows changes in $C(\tau)$ when the force amplitude f in (4) is increased.² As expected, the bottom panel, computed for the stationary flow, features an approximately log-periodic pattern, characteristic for systems with singular continuous spectrum [4]. The sequence of moderate (≈ 0.3) persistent peaks, with time intervals between subsequent peaks forming a growing geometric progression; the rightmost shown peak at $\tau \approx 25\,200$ corresponds to the average duration of $F_{19} = 4181$ rotations of a tracer around the torus. Increase of f leads to the formation of the oscillatory Eulerian component in the velocity and, hence, to disappearance of these peaks, starting at the large values of τ and gradually eroding the whole texture. The plots demonstrate that the original pattern of autocorrelation persists almost intact until a certain f -dependent threshold

²As already mentioned, we use here the rotation number equal to the inverse golden mean: at the true golden mean, the Andronov-Hopf bifurcation for the Eulerian variables is subcritical, hence transition to the Lagrangian chaos is abrupt. In contrast, in case of the inverse golden mean the bifurcation is supercritical. This ensures the gradual growth of the oscillation amplitude for the Eulerian velocity and allows us to visualize the fine details of the transition.

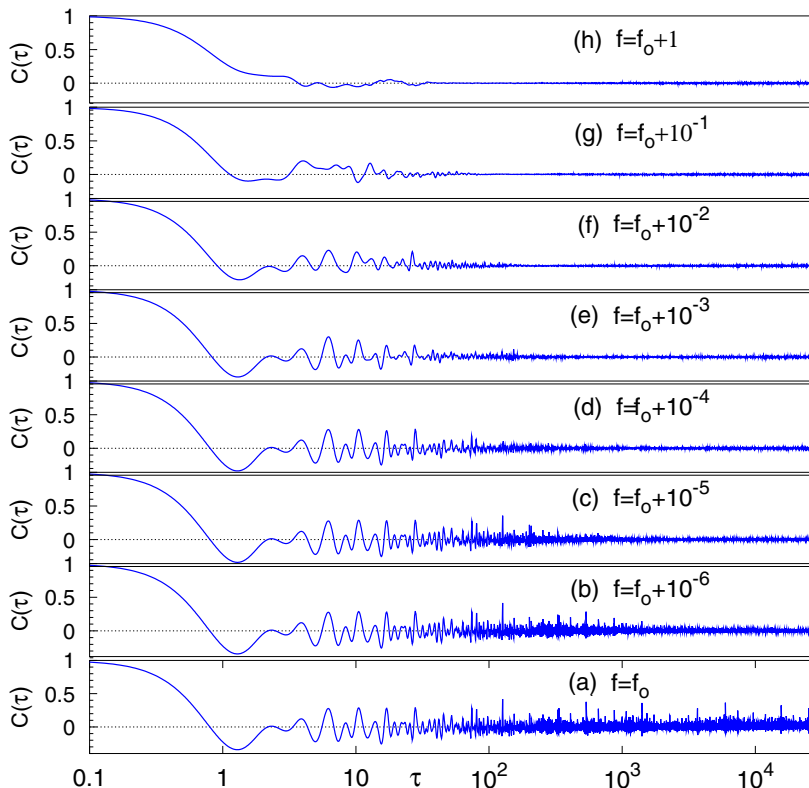


FIG. 4. Evolution of autocorrelation of velocity beyond the destabilization of the stationary flow pattern at f_0 . Parameter values: see Fig. 2.

value of τ ; beyond that value, autocorrelation rapidly decays. It is natural to call this threshold the “correlation horizon” c_h , and define it as the largest value of τ at which $|C(\tau)|$ assumes some moderate value c_0 . In other words, the correlation horizon corresponds to the length of the time interval, within which the bulk of the (now chaotically drifting) fluid particles still roughly reproduces the ordered motion along the streamlines of (now unstable) steady flow pattern. Beyond that time interval, denominators of the rational approximations to the rotation number of the steady flow cease to serve as time stamps for close returns of particles to their initial positions. Once departed from the stationary streamline, a generic chaotic tracer particle would not return to the scheduled motion along it. Of course, returns to the streamline itself happen now and then, but for different particles they occur at different times, and ensemble averaging effectively cancels the correlation. The further from the threshold f_0 , the shorter is the correlation horizon; in our calculations, we observe the power-law behavior $c_h(f) \sim (f - f_0)^{-0.4}$ [Fig. 3(b)].

Knowledge of the properties of the autocorrelation allows us to infer certain quantitative features of the power spectrum. In particular, composition of the spectral measure can be characterized in terms of the asymptotic properties of the “integrated autocorrelation” $C_{\text{int}}(T) = T^{-1} \int_0^T C(\tau)^2 d\tau$. The asymptotic value $C_{\text{int}}(\infty)$ is proportional to the weight of the discrete component in the spectral measure. Furthermore, in absence of the discrete component, the decay law of $C_{\text{int}}(T)$ at large T provides quantitative information on the continuous part of the spectrum: $C_{\text{int}}(T) \sim T^{-D_2}$ where D_2 is the (fractal) correlation dimension of the spectral measure [19].

Plots of $C_{\text{int}}(T)$, presented in Fig. 5, display for all values of $f \geq f_0$ the distinct decay by several orders of magnitude, allowing to conjecture that the discrete spectral component is completely

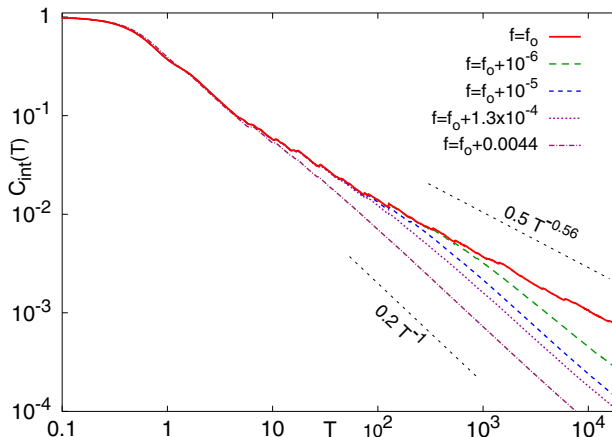


FIG. 5. Evolution of the integrated autocorrelation $C_{\text{int}}(T)$ close to the onset at f_o of the oscillatory instability of the stationary flow pattern. Parameter values: see Fig. 2.

absent. At $f = f_o$, $C_{\text{int}}(T)$ decays as $T^{-0.56}$, indicating that the continuous component of the spectrum is fractal (singular). At higher values of the forcing amplitude f this relatively slow decay is recognizable as an intermediate asymptotics, followed by the crossover to the faster ultimate decay $\sim 1/T$, as it should be expected for the absolutely continuous spectral measure.

VI. CONCLUSIONS

Summarizing, we have discussed metamorphoses in the power spectra of Lagrangian observables on the way from well ordered flow pattern to the developed Lagrangian chaos. Whereas for a chaotic motion the absolute continuity of the spectral measure is generally accepted, it is often implicitly expected that this motion inherits to the state with discrete spectrum. Focusing on the complementary case—the broad class of flows in which the Lagrangian spectra of prechaotic states are singular continuous—we illustrate in terms of the Fourier spectrum and autocorrelation function the transition from “nearly ordered” advection to Lagrangian chaos. We expect that similar changes should accompany the onset of time dependence in other flow patterns in which streamlines repeatedly return tracers into the arbitrarily small neighborhoods of stagnation points.

ACKNOWLEDGMENT

Our research has been supported by the DFG (Project No. ZA658/3-1) and RFBR (Project No. 20-51-12010).

-
- [1] V. I. Arnold, Sur la géométrie différentielle des groupes de Lie de dimension infinie et ses applications à l’hydrodynamique des fluides parfaits, *Ann. Inst. Fourier* **16**, 319 (1966).
 - [2] H. Aref, Stirring by chaotic advection, *J. Fluid Mech.* **143**, 1 (1984).
 - [3] T. Bohr, M. H. Jensen, G. Paladin, and A. Vulpiani, *Dynamical Systems Approach to Turbulence* (Cambridge University Press, Cambridge, 1998).
 - [4] A. S. Pikovsky, M. A. Zaks, U. Feudel, and J. Kurths, Singular continuous spectra in dissipative dynamics, *Phys. Rev. E* **52**, 285 (1995).
 - [5] J. P. Gollub and H. L. Swinney, Onset of turbulence in a rotating fluid, *Phys. Rev. Lett.* **35**, 927 (1975).
 - [6] J. P. Gollub and S. V. Benson, Many routes to turbulent convection, *J. Fluid Mech.* **100**, 449 (1980).

- [7] M. Reed and B. Simon, *Modern Methods of Mathematical Physics* (Academic Press, New York, London, 1972), Vol. 1.
- [8] S. Aubry, C. Godrèche, and J. M. Luck, A structure intermediate between quasi-periodic and random, *Europhys. Lett.* **4**, 639 (1987).
- [9] M. A. Zaks, A. S. Pikovsky, and J. Kurths, Steady viscous flow with fractal power spectrum, *Phys. Rev. Lett.* **77**, 4338 (1996).
- [10] L. D. Meshalkin and Ya. G. Sinai, Investigation of the stability of the stationary solution of a system of equations of plane viscous-fluid motion, *J. Appl. Math. Mech.* **25**, 1700 (1961).
- [11] N. F. Bondarenko, M. Z. Gak, and F. V. Dolzhansky, Laboratory and theoretical models of plane periodic flow, *Akademiia Nauk SSSR Fizika Atmosfery i Okeana* **15**, 1017 (1979).
- [12] J. Paret, D. Marteau, O. Paireau, and P. Tabeling, Are flows electromagnetically forced in thin stratified layers two dimensional? *Phys. Fluids* **9**, 3102 (1997).
- [13] D. Armbruster, B. Nicolaenko, N. Smaoui, and P. Chossat, Symmetries and dynamics for 2-D Navier-Stokes flow, *Physica D* **95**, 81 (1996).
- [14] J. Tithof, B. Suri, R. K. Pallantla, R. O. Grigoriev, and M. F. Schatz, Bifurcations in a quasi-two-dimensional Kolmogorov-like flow, *J. Fluid Mech.* **828**, 837 (2017).
- [15] I. I. Wertgeim, M. A. Zaks, R. V. Sagitov, and A. N. Sharifulin, Instabilities, bifurcations, and nonlinear dynamics in two-dimensional generalizations of Kolmogorov flow, *Fluid Dyn.* **57**, 430 (2022).
- [16] A. A. Nepomnyashchy, On the stability of secondary flows of viscous fluid in an unbounded space, *J. Appl. Math. Mech.* **40**, 836 (1976).
- [17] V. Rom-Kedar and S. Wiggins, Transport in two-dimensional maps, *Arch. Rational Mech. Anal.* **109**, 239 (1990).
- [18] R. V. Sagitov, I. I. Wertgeim, and M. A. Zaks (in preparation).
- [19] R. Ketzmerick, G. Petschel, and T. Geisel, Slow decay of temporal correlations in quantum systems with Cantor spectra, *Phys. Rev. Lett.* **69**, 695 (1992).